

Spliced Axially-Loaded Single-Angle Members in Compression

SHERIEF S. S. SAKLA, YOHANNA M. F. WAHBA, and MURTY K. S. MADUGULA

SUMMARY

Due to construction and transportation considerations, angles used as leg members in latticed towers are often joined together in the field using bolted splice plates. In many instances, the centroid of the angle cross section does not coincide with centroid of the splice plates used to connect the angles. It is not known what effect such a splice has on the compressive ultimate load carrying capacity of the single-angle member. Research results on spliced axially-loaded single-angle struts are not available in the literature. Results of compression tests on five spliced angle specimens of low slenderness ratio (fabricated according to the communication tower industry practice) and one reference specimen of the same size and length are reported herein and compared with AISC-LRFD Specification. It is shown that the ultimate load carrying capacity of spliced specimens was, on the average, 8% less than that of the reference specimen.

INTRODUCTION

Single angles are widely used in many structural applications. One important use of these structural members is as leg members or diagonals in transmission and communication towers. These towers can be self-supporting or guyed depending on the tower height and loading. To speed the construction procedure and minimize transportation cost and obstacles, a tower is divided into several sections suitable for transportation that are fabricated in the shop and then transported to the construction site where they are assembled together to erect the complete tower structure. It is a common practice in the communication tower industry to use bolted-splice plates instead of bolted splice angles for the leg splice to connect

different tower sections. These tower legs are usually designed as concentrically-loaded members since the angle is connected by both legs. In the panel where the legs of the tower are spliced, questions arise as to the effect of splicing on the compressive ultimate load carrying capacity and on the behavior of the angle legs. These leg members are usually of slenderness ratio that can be classified as stocky. A survey revealed that no research results are available in the published literature on the effect of splicing on the compressive resistance of axially-loaded single-angle struts.

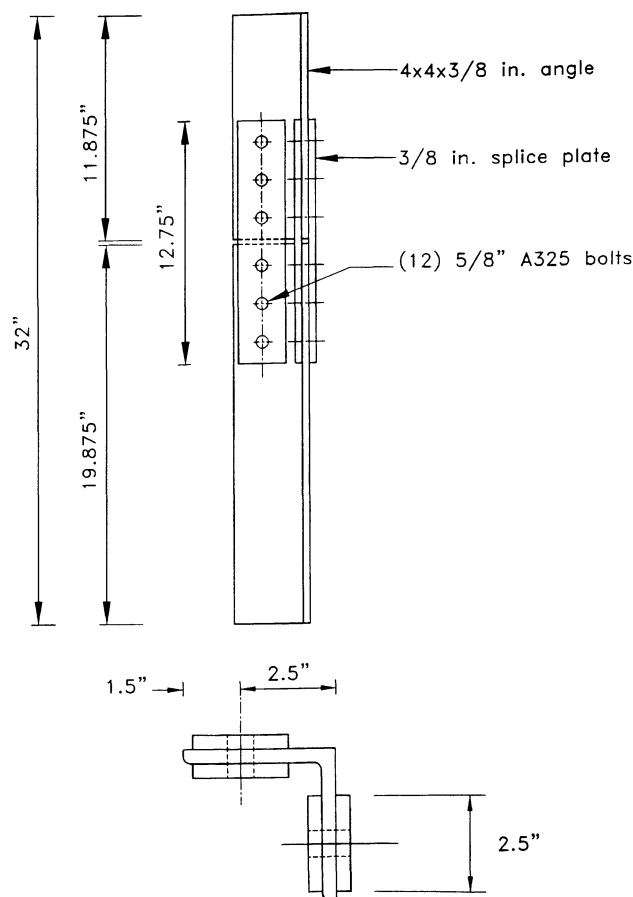


Fig. 1(a). Details of a typical test specimen

Sherief S.S. Sakla is Senior Design Engineer, Gala & Associates, Inc., Beverly Hills, Michigan.

Yohanna M.F. Wahba is Manager, Engineering, LeBlanc & Royle Telcom Inc., Oakville, Ontario, Canada.

Murty K.S. Madugula is Professor of Civil Engineering, Faculty of Engineering, College of Engineering and Science, University of Windsor, Windsor, Ontario, Canada.

To illustrate the problem, consider the spliced single-angle tower leg shown in Figure 1(a) and 1(b). Four $2\frac{1}{2} \times 12\frac{3}{4}$ in. splice plates of $\frac{3}{8}$ in. thickness are used for splicing a $4 \times 4 \times \frac{3}{8}$ in. angle. Thus the gross area of the splicing plates is 30% higher than that of the connecting angles. The $\frac{5}{8}$ in. bolts are spaced at two inches on each side of the connection. The gage distance is 2.5 in. while the edge distance is 1.5 in. This results in the minor principal axis of the spliced angle not coincident with the minor principal axis of the four splice plates. A question arises here regarding how to evaluate the load carrying capacity of the spliced axially-loaded angle.

Two different design practices are adopted by engineers when evaluating the ultimate load carrying capacity of such a member. In one practice, the cross sectional area of the splice plates is sized to be 1.25 times that of the angle gross area, hence the effect of the splice is neglected and the capacity is evaluated based on that of the axially-loaded single-angle strut. The simple-column equation of the AISC-LRFD,¹ AISC-ASD,² or any other design standard is used to find the ultimate load carrying capacity of the axially-loaded member for which the slenderness ratio, yield stress, and cross-sectional area are known. This is the practice that is generally followed by the communication tower industry in North America. The second practice is to evaluate the load that initiates yielding in the splice plates assuming that the single-angle column remains straight during the application of the load, thus ignoring any secondary stresses developed due to the deflected shape of the angle under the applied load. This practice is generally followed in Europe.

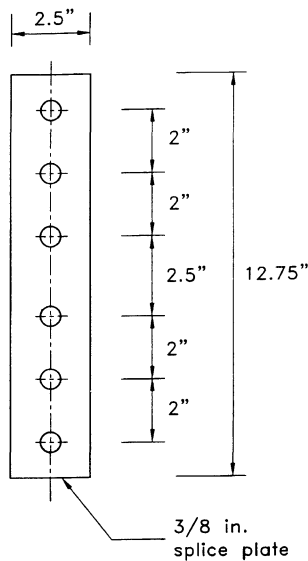


Fig. 1(b). Details of a typical splice plate

Referring to Figure 2, it can be seen that the minor principal axis of the angle, the z axis, does not coincide with the minor principal axis of the four splice plates, the z' axis. As the angle is loaded concentrically, this load is transferred eccentrically to the splice plates. The value of this eccentricity is 0.291 in. for the connection shown in Figures 1(a) and 1(b). The eccentricity of the load with respect to the splice plates results in the stress distribution shown in Figure 2. Thus for a compression load of P kips, the maximum compression stress of $0.562P$ ksi occurs in the outer splice plate near the angle heel. If the splice plates have a yield stress of 36 ksi, a load of 64.1 kips (i.e., $36/0.562$) will initiate yielding of the splice plate assuming that the angle strut remains straight during loading. This will be the compressive capacity of the splice as per the European practice. If the angle member has a yield stress of 50 ksi, and the buckling length is 34 in., which was the length of the specimens used in this investigation, the ultimate load carrying capacity of the axially-loaded column according to AISC-LRFD¹ is 124.8 kips using a resistance factor, ϕ , of 1.0. This would be the capacity of the splice as per the North American practice. Thus, a great difference exists between the two practices for calculating the maximum compressive strength. The difference increases as the slenderness ratio of the angle member decreases and/or the eccentricity between the z -axis and z' -axis increases.

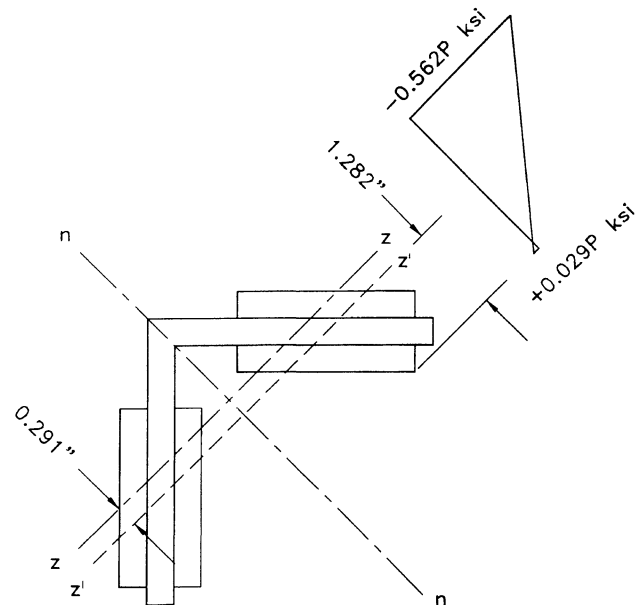


Fig. 2. Stress distribution in the splice plates according to the beam theory

EXPERIMENTAL PROGRAM

Test Specimens

An experimental program was carried out to study the effect of splicing on the behavior and ultimate load carrying capacity of axially-loaded single-angle members. The experimental program consisted of six ultimate strength tests of axially-loaded single angles. A typical test specimen is shown in Figure 1(a) and 1(b). In order to reduce the number of variables in this study, the same size angle was used for all tests. The angle length was kept at 32 in. This resulted in a buckling length of 34 in. and a slenderness ratio of 43. A typical spliced test specimen consisted of two pieces of $4 \times 4 \times \frac{3}{8}$ in. single angle made of ASTM Grade 50 steel. The two angle pieces were connected together using four Grade A36 splice plates. Twelve $\frac{5}{8}$ in. A325 bolts pretensioned to a 150 lb-in. torque (which represents a snug-tight condition) were used in the connection. As shown in Figure 1(a), there was a clearance of $\frac{1}{4}$ in. between the two angles comprising the specimen. Four specimens of this configuration, designated S-1, S-2, S-3, and S-5, were fabricated and tested. A fifth specimen, designated S-4, of the same configuration as S1, S2, S3, and S5 was tested after the clearance between the connected angles was filled with two steel packing bars of $\frac{1}{4} \times \frac{1}{4} \times 4$ in. A $4 \times 4 \times \frac{3}{8}$ in. angle of 32 in. length, designated S-6, was tested to be used as a reference specimen for comparison purposes.

Each of the test specimens was then machined at both ends to ensure that the ends were perfectly square and parallel to each other. For all the specimens, four strain gages were attached at a distance of 7 in. from bottom as shown in Figure 5. These were attached to help ensure concentric axial loading of the angle. To study the behavior of the splice plates at the gap between the two angles, six strain gages were attached to the splice plates of specimen S2, as shown in Figure 5. In order to detect the yielding pattern during loading, all the specimens were coated with a thin layer of white wash before testing and allowed to dry. This brittle coating that flaked off at the points of yielding exposing the steel surface below, provided a very economical solution for detecting high-yielding zones.

Test Procedure

All the tests were carried out using a 200 kip capacity test frame in the Structures Laboratory at the University of Windsor. Details of the test setup are shown in Figure 3 and 4. Hinged end conditions were created at the ends of the specimens. Ball and socket joints at the ends of the base and top plates were used to facilitate transfer of concentric axial load to the angles being tested. These end fixtures were designed to permit rotations about the three

global axes at the ends of the specimen. At the base of the specimen, the load was applied using a 200-kip capacity hydraulic jack and a hand-operated pump. A Strainsert calibrated flat load cell with a digital readout gage was used to obtain direct load measurements. Two dial gages at mid-height of the specimen, as illustrated in Figure 4, were used to measure lateral deflections.

Each specimen was loaded up to about 10 kips and the strain gage readings were taken. The load was then released to almost zero and the specimen was then adjusted to eliminate any eccentricity. The same procedure was repeated several times until the load was concentric. In all cases the test proceeded when the applied load was concentrically applied to the specimen causing the four strain gage readings to be within 5% of each other. Figure 4 shows specimen S-6 in place ready to be tested. The white-washed specimen, the hydraulic jack, the lower and upper plates, and the test frame can be seen in that figure. A visual inspection of the cracks developed in the white-wash was made throughout the tests. The mode of failure was determined, recorded, and photographed. In all

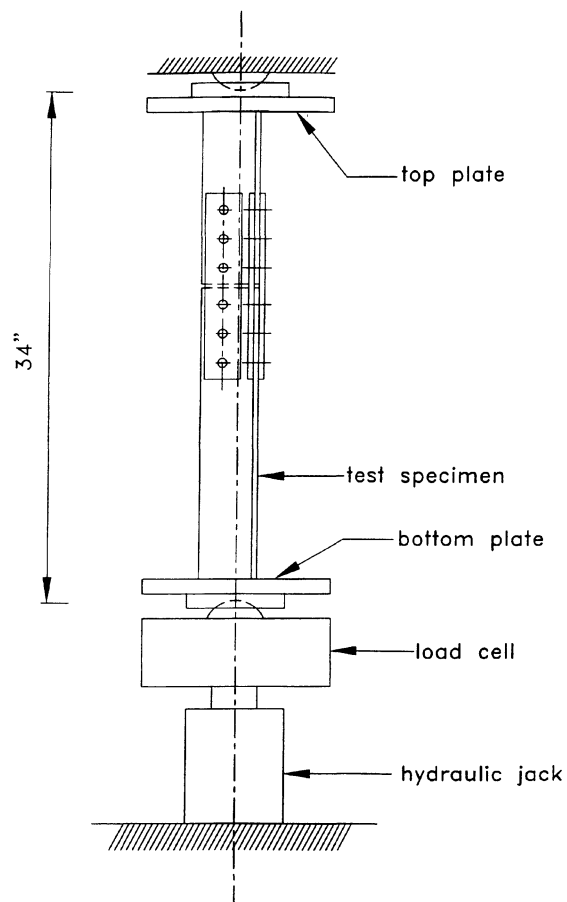


Fig. 3. Test setup

cases, before reading the strain gages at a given load level, the system was allowed to reach equilibrium, which was assumed to be the point at which the load cell and strain gage readings had stopped changing. In all tests, the failure load was determined to be the maximum recorded load with no further possible increase in load. A typical test took an average of two hours to complete both the setup and testing.

Mechanical Properties

In order to determine the yield stress, four tension tests were conducted on coupons taken from the same stock as that of the test specimens. Two were taken from the angle and the other two from the splice plates. The specimens were prepared according to the ASTM E8-89,³ but their dimensions were adapted to suit the dimensions of the angles and the grips of the testing machine. The thicknesses of the specimens were the same as those of the angles and plates. The tension tests were carried out in a 300 kN Tinius Olsen Universal Testing Machine. The average yield stress of the angles was found to be 52.8 ksi. For the splice plates, the average yield stress was 43.5 ksi.

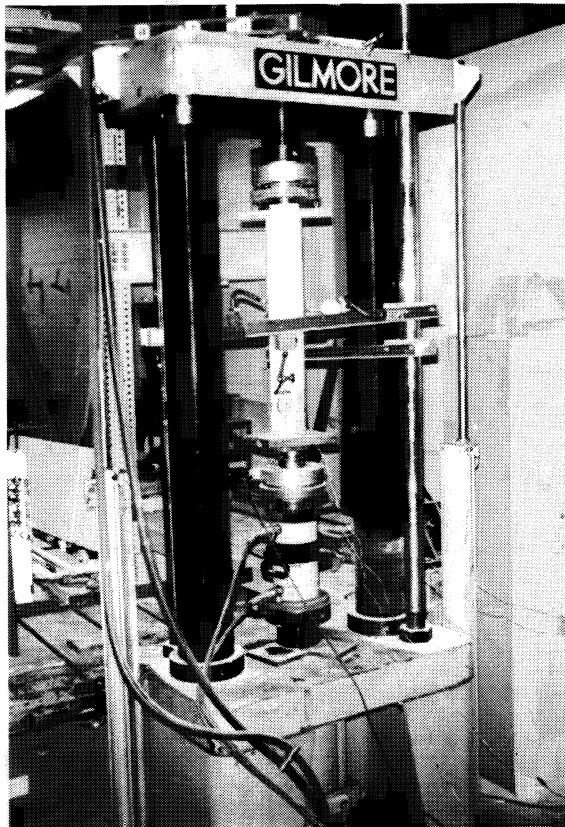


Fig. 4. Test setup for Specimen S-6

These values were used in all theoretical computations of the failure loads of test specimens.

Failure Mode

The maximum load carrying capacities of the angle test specimens are shown in Table 1. All the specimens showed the typical mode of failure observed in testing very short columns. Lateral deflections were very small at the beginning of loading and did not have a certain direction. Increasing the applied load caused the bolts to slip. The first sound of slipping was heard at a load level between 30 and 37 kips for Specimens S-1, S-2, S-3, and S-5 and at a load level of 43 kips for Specimen S-4. For Specimens S-1, S-2, S-3, and S-5, the white-wash started flaking at the outer splice plates near the heel of the angle, as predicted, at a load level of 83 to 89 kips. The cracks in the white-wash started propagating toward the center of the splice plates and toward the splice ends and cracks

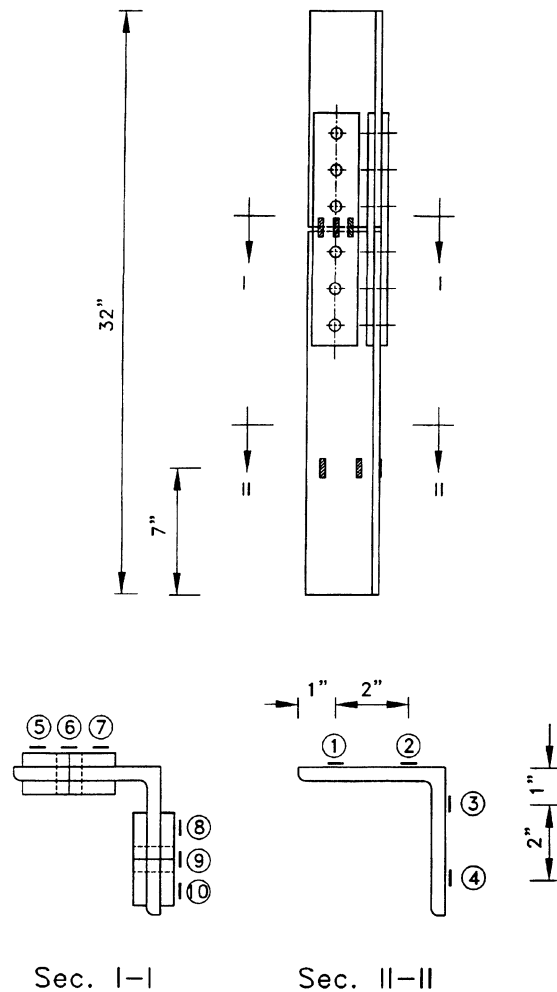


Fig. 5. Location of strain gages

started also showing around the bolts (i.e. cracks started propagating in all directions). At about 90% of the failure load, horizontal cracks in the white-wash were visible at the toes of the angle, especially at the ends. This was due to the excessive deformation of the splice plate which caused the gap between the angles to close at the heel and open at the toes, causing more compression to flow towards the heel of the angle at the splice location but more uniform towards the ends. At failure, the ends of the angle were completely squashed as was indicated by the flaking of the white-wash at the ends of the specimens. A typical crack pattern is shown in Figure 6 for specimen S-1. As can be seen from that figure, the angle was bent due to closure of the gap near the heel and the opening of the gap near the toes. Figure 7 is a close-up view of the outer splice plates for specimen S-1. The flaked white-wash can be seen at the mid-length of the splice plate. As expected, the yield zone was much longer on the side of the splice plate towards the heel of the angle. The squashing of the angle legs at the ends can also be seen.

For Specimen S-4 with packing bars, the maximum load carrying capacity was 121.0 kips as given in Table 1. The failure mode was basically the same as specimens S-1, S-2, S-3, and S-5 except that there was no excessive flaking of the white-wash in the splice plates. The white-wash started flaking at the outer splice plates near the heel at a load of about 74 kips. No further flaking of the white-wash was noticed after the initial flaking. At about 90% of the failure load, horizontal cracks in the white wash were visible at the toes of the angle along the entire length. More white-wash cracks were visible at the ends of the specimen indicating a squashing pattern although no propagation of cracks in the splice plates was observed. The

reference specimen, S-6, failed at a load of 125.2 kips as given in Table 1. Horizontal cracks at the ends of the angle were noticed at a load of 110 kips indicating squashing of

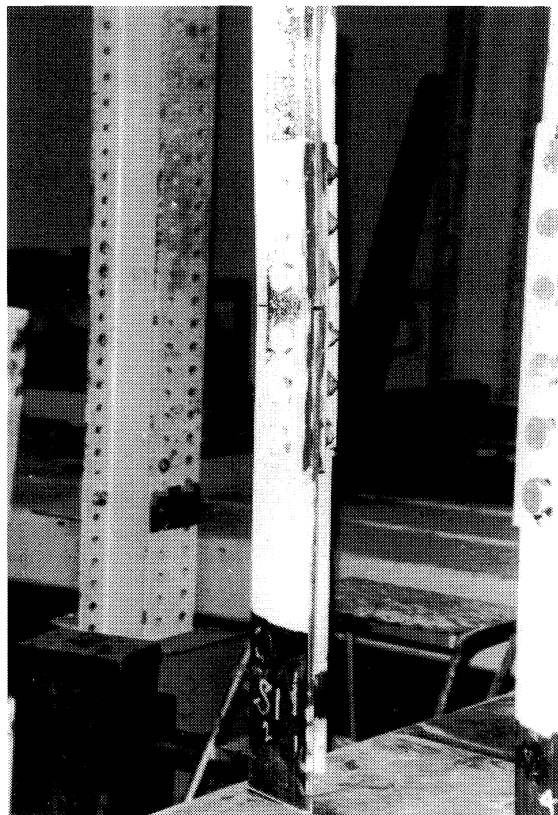


Fig. 6. Typical crack pattern (Specimen S-1)

Test Specimen I.D. (1)	Maximum Compressive Load Carrying Capacity (kips) (2)	Average (kips) (3)	Ratio with Respect to a Non-Spliced Angle (4)
S-1	117.7	115.0	0.92
S-2	105.0		
S-3	122.3		
S-5	115.0		
S-4 ^a	121		0.97
S-6 ^b	125.2		1

^aPacking bars were used between the spliced angles.
^bReference specimen—one piece of angle without any splice plates.

the angle ends as shown in Figure 8. Horizontal cracks were visible at the toes of the angle along the entire length. Cracks continued propagating towards the heel all over the entire length of the specimen.

Figures 9 to 11 show, for load levels of 10, 20, and 60 kips respectively, a comparison between the stresses obtained from the experimental strains ($E\varepsilon$) and the stresses calculated using the beam theory assuming that the load is applied through the centroid of the angle. At a load level of 10 kips, a reasonable agreement existed between the experimentally measured stresses and the beam theory. At that level the lateral deflections were very minimal. As the load increased, the angle struts started to buckle and the eccentricity of the load with respect to the splice plates increased as the angle cross-section shifted. It can be seen from Figures 9 to 11 that as the load increased there was less agreement between the experimental stresses and stresses according to the beam theory. After the splice plates yielded, the gap at the heel of the angles closed and the load eccentricity with respect to the splice plates increased.

DISCUSSION

Section M3 of the AISC-LRFD Specification – 1993, as well as the 1989 AISC-ASD specification, requires that

the column compression joints at splice or at base plates should keep the gap to $\frac{1}{16}$ in. or less. If the gap exceeds $\frac{1}{16}$ in. but is less than $\frac{1}{4}$ in., and if an engineering investigation shows that sufficient contact area does not exist, the gap should be packed out with non-tapered steel shims. Gaps $\frac{1}{4}$ in. and over are not covered by AISC specifications. In the present investigation, four of the five specimens had a uniform gap of $\frac{1}{4}$ in., which is the practice in the communication tower industry. Thus a lower capacity of the spliced specimens (average 115 kips) is expected as compared to the spliced specimen with shims provided (121 kips). At 90% of the failure load, excessive deformations of the splice plates caused the gap between the angles to close at the heel and open at the toe, causing more secondary bending effects.

In transmission tower leg design, the compression splice for the leg angle is sized to have a cross-sectional area 1.25 times that of the angle leg. In the present investigation, the ratio of the gross area of the splice plates to the angle gross area is 1.31 (i.e., $3.75/2.86$) and the ratio of the yield stress of the splice plates to the yield stress of the angle is 0.82 (i.e., $43.5/52.8$). Thus the capacity of the splice plates in compression yielding is 1.08 times that of the

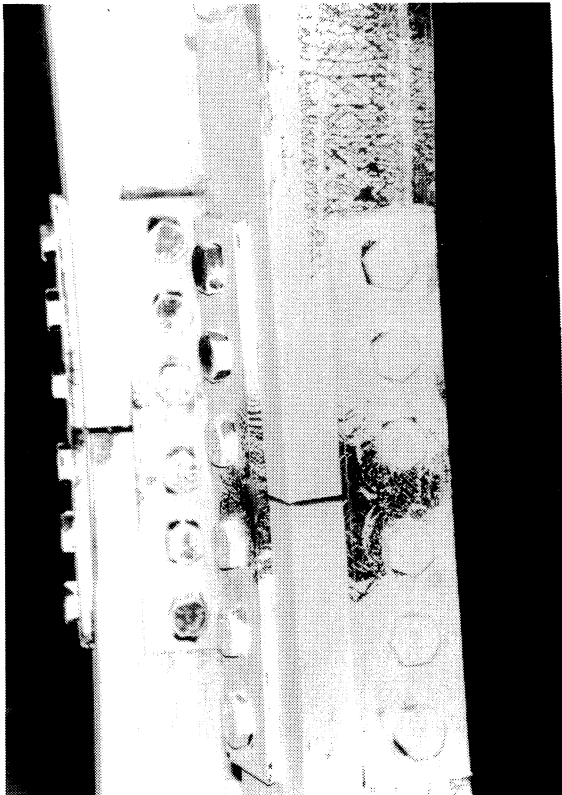


Fig. 7. Close-up view of outer splice plates (Specimen S-1)

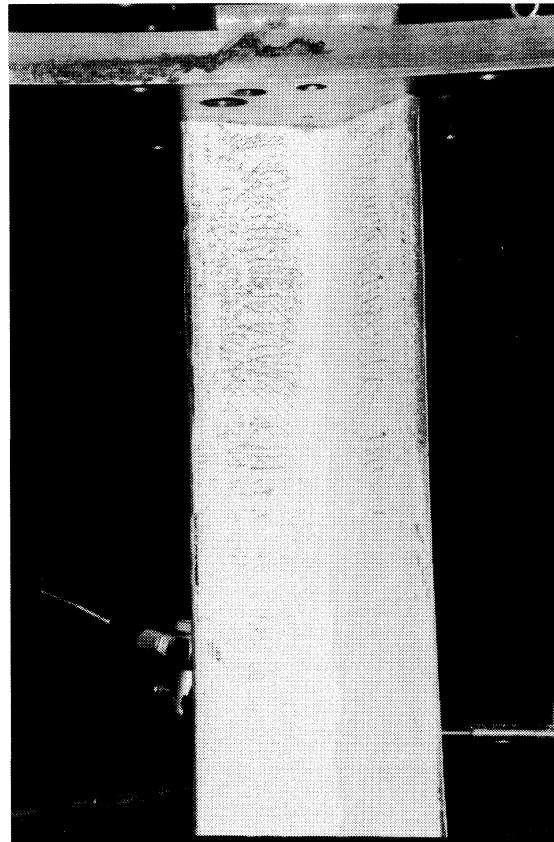


Fig. 8. Crack pattern at the top of Specimen S-6

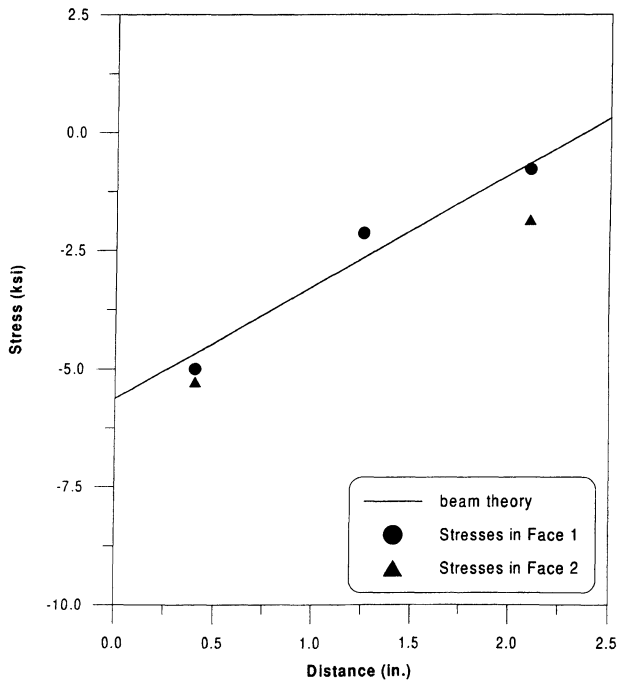


Fig. 9. Stress distribution at mid-length of splice plates at a load level of 10 kips.

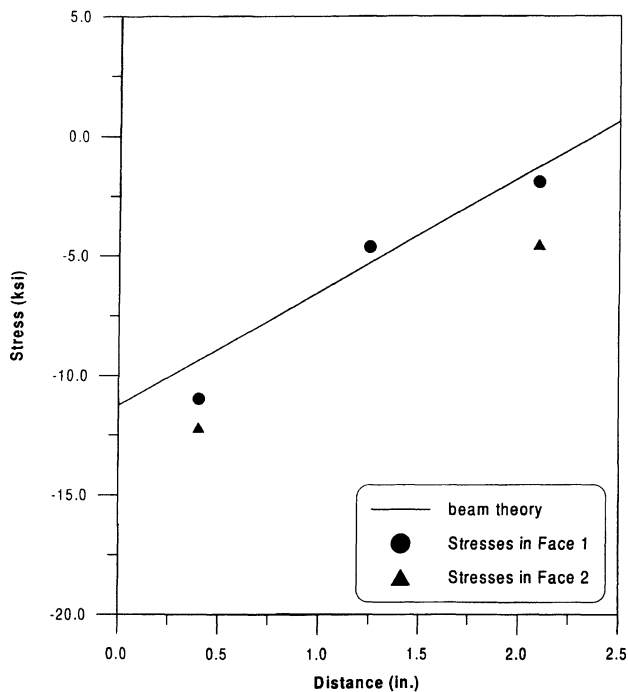


Fig. 10. Stress distribution at mid-length of splice plates at a load level of 20 kips.

angle (i.e., 3.75 x 43.5 versus 2.86 x 52.8). This is less than 1.25 required as per the transmission tower design practice. However, the specimens were fabricated in conformity with the communication tower industry practice. It is desirable to eliminate the eccentricity in the splice by changing the gage distance of the bolts or changing the width of the outer splice plates. The use of angles, instead of plates, to form the splices may also reduce the eccentricity.

CONCLUSIONS AND RECOMMENDATIONS

For the conditions of the experimental investigation reported herein, the following conclusions can be drawn:

- (1) There is no significant decrease in the ultimate load carrying capacity of axially-loaded spliced single-angles when compared with axially-loaded one-piece angles.
- (2) The initiation of yielding was always in the mid-length of the splice plate.
- (3) Using packing bars between the two pieces of the spliced angles did not have a significant effect on the maximum compressive load carrying capacity.

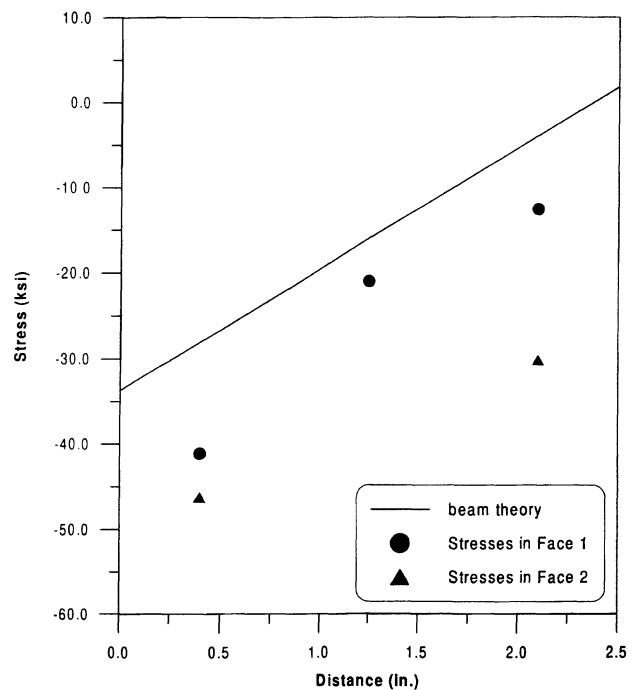


Fig. 11. Stress distribution at mid-length of splice plates at a load level of 60 kips.

REFERENCES

1. American Institute of Steel Construction, Inc., *Load and Resistance Factor Design Manual of Steel Construction*, 2nd Edition, Chicago, IL, 1994.
2. American Institute of Steel Construction, Inc., *Allowable Stress Design Manual of Steel Construction*, 9th Edition, Chicago, IL, 1989.
3. American Society for Testing and Materials, *Metals*

Test Methods and Analytical Procedures, Section Vol. 03.01, pp. 131-161, Philadelphia, 1989.

NOTATION

$z - z$ = minor principal axis of angle cross section
 $z' - z'$ = minor principal axis of the splice plates
 ϕ = resistance factor